Y. Wiaux, J. D. McEwen, and P. Vielva

Complex Data Processing: Fast Wavelet Analysis on the Sphere

Y. Wiaux, J. D. McEwen, and P. Vielva

Communicated by Jean-Pierre Antoine

ABSTRACT. *In the general context of complex data processing, this article reviews a recent practical approach to the continuous wavelet formalism on the sphere. This formalism notably yields a correspondence principle which relates wavelets on the plane and on the sphere. Two fast algorithms are also presented for the analysis of signals on the sphere with steerable wavelets.*

1. Introduction

In many fields of science, from computer vision, to biomedical imaging, geophysics, or astrophysics and cosmology, experiments are set up releasing more and more complex data to process. A first complexity of the data lies in their large volume, related to the always increasing resolution of technological devices. Moreover, data are not necessarily distributed on the real line (audio signals, . . .), or on the plane (images, . . .), but can live on higher-dimensional or nontrivial manifolds ($\mathbb{R}^n$, sphere, hyperboloid, . . .). Finally, the data may correspond not only to scalar fields (local intensity), but also to tensor fields on those manifolds (local diffusion matrix, local polarization, . . .).

In this new era of complex data processing, powerful tools always need to be developed for the precise analysis of the signals under scrutiny. In this article, we review recent formal and algorithmic advances for the continuous wavelet analysis of signals on the sphere. This scale-space formalism goes well beyond the spectral analysis, as it enables one to probe the localization, scale, and orientation of the features of the signals analyzed. An exhaustive

review on wavelets on the sphere and related manifolds is presented in another article of the present issue [5].

For the sake of the illustration we choose the example of the cosmic microwave background (CMB) data from cosmology. The CMB is a polarized electromagnetic blackbody radiation observed today in all directions of the sky, which emerged some 380.000 years after the Big Bang. This snapshot of the early universe bears a wealth of information for the study of its structure and evolution, i.e., for cosmology. The present NASA WMAP (*Wilkinson Microwave Anisotropy Probe*) satellite experiment [6] releases maps of the celestial sphere of 3 megapixels at each detection frequency, while the forthcoming ESA Planck Surveyor satellite experiment [24] will increase the resolution to 50 megapixels. The CMB therefore crystallises the previously quoted potential data complexities. Its temperature (intensity) and polarization, respectively, define scalar and tensor fields on the sphere, and the corresponding experimental data already appear in large volumes. Various applications of the continuous wavelet formalism on the sphere for the analysis of the CMB are presented in another article of the present issue [23].

The structure of the article goes as follows. We only focus on the formalism for the continuous wavelet transform on the sphere introduced in [2], as recently further developed in a practical approach by [29]. This formalism is explicitly reviewed in Section 2. The wavelet decomposition of a signal on the sphere S^2 is defined by its projection coefficients on translated, rotated, and dilated versions of a mother wavelet, i.e., a directional correlation at each analysis scale. These wavelet coefficients therefore live on the rotation group in three dimensions $SO(3)$. The wavelet must satisfy an admissibility condition ensuring that the signal may be explicitly reconstructed from its wavelet coefficients. A correspondence principle is also recalled stating that wavelets on the sphere may be built from an inverse stereographic projection of wavelets on the plane. This principle enables one to transfer onto the sphere some properties of wavelets on the plane, such as the notion of steerability. We explicitly describe major examples of axisymmetric, directional, and steerable wavelets. In Section 3, we give the generic definition of directional correlation, and the definition of standard correlation, to which reduce the wavelet coefficients of a signal with a steerable or axisymmetric wavelet. We discuss their *a priori* computation cost on any pixelization of S^2 and of $SO(3)$, which is prohibitive for high resolution data. We emphasize the existence of a directional and standard correlation relation in harmonic space. In Section 4, we first discuss the band-limitation of signals and filters. We then review two fast algorithms for the directional correlation of band-limited signals and filters on iso-latitude pixelizations on the sphere. The first one is based on a technique of separation of variables in the Wigner D-functions on $SO(3)$ [18, 30]. The second one relies on the factorization of the three-dimensional rotation operators to interpret the result of the directional correlation as a function on the three-torus $\mathbb{T}^3$, and applies the separation of variables to three-dimensional imaginary exponentials [25, 28, 22]. The *a priori* $\mathcal{O}(L^5)$ asymptotic complexity is thereby reduced to $\mathcal{O}(L^4)$, where $2L$ roughly stands for the square-root of the number of pixels on the sphere, i.e., for band-limited signals and filters with band-limit $L \in \mathbb{N}$. For steerable and axisymmetric wavelets, the directional correlation resumes to standard correlations, and the asymptotic complexity drops to $\mathcal{O}(L^3)$. The typical computation time for the directional correlation of megapixels maps ($L \simeq 10^3$) correspondingly drops from years to tens of seconds on a standard computer. This easily allows the analysis of multiple signals at such high resolutions, and at multiple scales. These developments finally lead us to our conclusions in Section 5.

2. Continuous Wavelets on the Sphere

2.1 Practical Approach

Among other approaches [17, 11, 12], a satisfactory formalism for the continuous wavelet transform of signals on the sphere S^2 was originally established in a group-theoretical framework [2, 3, 4, 9, 7]. The aim of the present article is to review a more practical but completely equivalent approach, recently proposed by [29]. In that framework, a "mother wavelet" $\Psi(\omega)$ is defined as a localized square-integrable function on the unit sphere, on which continuous affine transformations (translations, rotations, and dilations) may be applied. The wavelet transform of a square-integrable signal on the sphere is then defined as the directional correlation of the signal with the dilated versions of the mother wavelet. At each scale, the corresponding wavelet coefficients are square-integrable functions on the rotation group in three dimensions $SO(3)$. Finally, an admissibility condition is imposed on the wavelet which ensures an exact reconstruction formula of the signal from its wavelet coefficients.[1]

The real and harmonic structures of the unit sphere S^2 are concisely summarized as follows. Any point ω on the sphere is given in spherical coordinates as $\omega = (\theta, \varphi)$, in terms of a polar angle, or co-latitude $\theta \in [0, \pi]$, and an azimuthal, or longitudinal angle $\varphi \in [0, 2\pi[$. Let $G(\omega)$ be a square-integrable function on the sphere, i.e., $G(\omega)$ in $L^2(S^2, d\Omega)$, with the invariant measure $d\Omega = d\cos\theta \, d\varphi$. The spherical harmonics form an orthonormal basis for the decomposition of functions in $L^2(S^2, d\Omega)$. They are explicitly given in a factorized form in terms of the associated Legendre polynomials $P_l^m(\cos\theta)$ and the complex exponentials $e^{im\varphi}$ as

$$Y_{lm}(\theta, \varphi) = \left[\frac{2l+1}{4\pi} \frac{(l-m)!}{(l+m)!} \right]^{1/2} P_l^m(\cos\theta) \, e^{im\varphi} , \qquad (2.1)$$

with $l \in \mathbb{N}$, $m \in \mathbb{Z}$, and $|m| \leq l$ [1, 27]. While the index l represents an overall frequency on the sphere, $|m|$ represents the frequency associated with the azimuthal variable φ. Any $G(\omega)$ is thus uniquely given as a linear combination of scalar spherical harmonics $G(\omega) = \sum_{l \in \mathbb{N}} \sum_{|m| \leq l} \widehat{G}_{lm} Y_{lm}(\omega)$ (inverse transform), for the scalar spherical harmonics coefficients $\widehat{G}_{lm} = \int_{S^2} d\Omega \, Y_{lm}^*(\omega) G(\omega)$ (direct transform), with $|m| \leq l$.

The continuous affine transformations on functions on the sphere are defined as follows. The operator $R(\omega_0)$ for the motion, or translation, of amplitude $\omega_0 = (\theta_0, \varphi_0)$ of a function reads

$$[R(\omega_0) G](\omega) = G\left(R_{\omega_0}^{-1}\omega\right) , \qquad (2.2)$$

where $R_{\omega_0}(\theta, \varphi) = [R_{\varphi_0}^{\hat{z}} R_{\theta_0}^{\hat{y}}](\theta, \varphi)$ is defined by the three-dimensional rotation matrices $R_{\theta_0}^{\hat{y}}$ and $R_{\varphi_0}^{\hat{z}}$, acting on the Cartesian coordinates (x, y, z) in three dimensions centered

---

[1] Notice that the signals and filters considered by the formalism are scalar functions, i.e., invariant under local rotations in the tangent plane at each point on the sphere. In the general context of complex data processing, one might want to generalize the wavelet formalism presented here to the analysis of rank n tensor functions. However, tensor fields may equivalently be expressed in terms of scalar fields. In particular, polarization data on the sphere constitute a rank 2 tensor field. It can be equivalently described in terms of its so-called electric and magnetic parts, which actually constitute two separate functions on the sphere, with a purely scalar behavior. The present formalism for the scale-space wavelet decomposition of scalar functions on the sphere may therefore be applied to the analysis of both scalar fields, and tensor fields such as polarization data [30, 31].

on the sphere and associated with $\omega = (\theta, \varphi)$. The rotation operator $R^{\hat{z}}(\chi)$ of a function around itself, by an angle $\chi \in [0, 2\pi[$, is given as

$$\left[R^{\hat{z}} (\chi) \, G \right] (\omega) = G \left(R^{\hat{z}\,-1}_{\chi} \omega \right) \, , \tag{2.3}$$

where $R^{\hat{z}}_{\chi}(\theta, \varphi) = (\theta, \varphi + \chi)$ also follows from the action of the three-dimensional rotation matrix $R^{\hat{z}}_{\chi}$ on the Cartesian coordinates (x, y, z) associated with $\omega = (\theta, \varphi)$. The dilation operator $D(a)$ on functions in $L^2(S^2, d\Omega)$, for a dilation factor $a \in \mathbb{R}^*_+$, is defined in terms of the inverse of the corresponding dilation D_a on points in S^2 as

$$[D(a) \, G] (\omega) = \lambda^{1/2} (a, \theta) \, G \left(D_a^{-1} \omega \right) \, , \tag{2.4}$$

with $\lambda^{1/2}(a, \theta) = a^{-1}[1 + \tan^2(\theta/2)]/[1 + a^{-2} \tan^2(\theta/2)]$. The dilated point is given by $D_a(\theta, \varphi) = (\theta_a(\theta), \varphi)$ with the linear relation $\tan(\theta_a(\theta)/2) = a \tan(\theta/2)$. The dilation operator therefore maps the sphere without its South pole on itself: $\theta_a(\theta) : \theta \in [0, \pi[\rightarrow \theta_a \in [0, \pi[$. This dilation operator is uniquely defined by the requirement of the following natural properties [29]. The dilation D_a of points on S^2 must be a radial (i.e., only affecting the radial variable θ independently of φ, and leaving φ invariant) and conformal (i.e., preserving the measure of angles in the tangent plane at each point of S^2) diffeomorphism (i.e., a continuously differentiable bijection on S^2). The factor $\lambda(a, \theta)$ explicitly appears in the conformal transformation of the metric through the dilation D_a. The normalization by $\lambda^{1/2}(a, \theta)$ in (2.4) is uniquely determined by the requirement that the dilation $D(a)$ of functions in $L^2(S^2, d\Omega)$ be a unitary operator (i.e., preserving the scalar product in $L^2(S^2, d\Omega)$, and specifically the norm of functions).

The analysis of signals goes as follows. The wavelet transform of a signal $F(\omega)$ in $L^2(S^2, d\Omega)$ on the sphere, with the wavelet $\Psi(\omega)$, localized analysis function in $L^2(S^2, d\Omega)$, is defined as the directional correlation between $F(\omega)$ and the dilated wavelet $\Psi_a = D(a)\Psi$, i.e., as the scalar product:

$$W_{\Psi}^F (\rho, a) = \langle \Psi_{\rho,a} | F \rangle = \int_{S^2} d\Omega \, \Psi_{\rho,a}^* (\omega) \, F (\omega) \, , \tag{2.5}$$

with $\Psi_{\rho,a} = R(\rho)\Psi_a$, and $\rho = (\theta_0, \varphi_0, \chi)$. At each scale, the wavelet coefficients $W_{\Psi}^F(\rho, a)$ are therefore square-integrable functions on the rotation group in three dimensions $SO(3)$. They represent the characteristics of the signal for each analysis scale a, direction χ, and position ω_0. This defines the scale-space nature of the wavelet decomposition on the sphere.

The real and harmonic structures of the rotation group in three dimensions $SO(3)$ are concisely summarized as follows. Any rotation ρ on $SO(3)$ is given in terms of the three Euler angles $\rho = (\theta, \varphi, \chi)$, with $\theta \in [0, \pi]$, and $\varphi, \chi \in [0, 2\pi[$. Let $H(\rho)$ be a square-integrable function on $SO(3)$, i.e., $H(\rho)$ in $L^2(SO(3), d\rho)$, with the invariant measure $d\rho = d\varphi d \cos \theta d\chi$. The Wigner D-functions are the matrix elements of the irreducible unitary representations of weight l of the group in $L^2(SO(3), d\rho)$. By the Peter-Weyl theorem on compact groups, the matrix elements D_{mn}^{l*} also form an orthogonal basis in $L^2(SO(3), d\rho)$. They are explicitly given in a factorized form in terms of the real Wigner d-functions $d_{mn}^l(\theta)$ and the complex exponentials, $e^{-im\varphi}$ and $e^{-in\chi}$, as

$$D_{mn}^l (\varphi, \theta, \chi) = e^{-im\varphi} d_{mn}^l (\theta) \, e^{-in\chi} \, , \tag{2.6}$$

with $l \in \mathbb{N}$, $m, n \in \mathbb{Z}$, and $|m|, |n| \leq l$ [27, 8]. Again, l represents an overall frequency on $SO(3)$, and $|m|$ and $|n|$ the frequencies associated with the variables φ and χ, respectively. Any $H(\rho)$, such as the wavelet coefficients at each scale of a signal on S^2, is thus uniquely given as a linear combination of Wigner D-functions as $H(\rho) = \sum_{l \in \mathbb{N}} (2l + 1)/8\pi^2 \sum_{|m|,|n| \leq l} \widehat{H}_{mn}^l D_{mn}^{l*}(\rho)$ (inverse transform), with, for $|m|, |n| \leq l$, the Wigner D-functions coefficients $\widehat{H}_{mn}^l = \int_{SO(3)} d\rho \, D_{mn}^l(\rho) H(\rho)$ (direct transform).

The synthesis of a signal $F(\omega)$ from its wavelet coefficients reads as:

$$F(\omega) = \int_0^{+\infty} \frac{da}{a^3} \int_{SO(3)} d\rho \, W_\Psi^F(\rho, a) \left[R(\rho) L_\Psi \Psi_a\right](\omega) . \tag{2.7}$$

In this relation, the operator L_Ψ in $L^2(S^2, d\Omega)$ is defined [2] by the following action on the spherical harmonics coefficients of functions: $\widehat{L_\Psi G}_{lm} = \widehat{G}_{lm}/C_\Psi^l$, with $|m| \leq l$. This exact reconstruction formula holds if and only if the spherical harmonics transform $\widehat{\Psi}_{lm}$ of the wavelet $\Psi(\omega)$ satisfies the following admissibility condition [29]:

$$0 < C_\Psi^l = \frac{8\pi^2}{2l + 1} \sum_{|m| \leq l} \int_0^{+\infty} \frac{da}{a^3} \left|(\widehat{\Psi_a})_{lm}\right|^2 < \infty , \tag{2.8}$$

for all $l \in \mathbb{N}$. This condition intuitively requires that the whole wavelet family $\Psi_a(\omega)$, for $a \in \mathbb{R}_+^*$, covers each frequency index l with a finite and non-zero amplitude. As explicitly expressed in Section 3, the direct Wigner D-functions transform of the wavelet coefficients of a signal F with Ψ is given as the pointwise product of the spherical harmonics coefficients $\widehat{F}_{lm}$ and $(\widehat{\Psi_a})_{ln}^*$. The admissibility condition consequently requires that the wavelet family as a whole preserves the signal information at each frequency l.

2.2 Correspondence Principle

Wavelets on the plane are well-known, and may be easily constructed as the corresponding admissibility condition reduces to a zero-mean condition for a function both integrable and square-integrable. On the contrary, the admissibility condition (2.8) for wavelets on the sphere is difficult to check in practice. In that context, a correspondence principle was proved in [29], stating that the inverse stereographic projection of a wavelet on the plane leads to a wavelet on the sphere.

The stereographic projection is the unique radial conformal diffeomorphism mapping the sphere S^2 onto the plane $\mathbb{R}^2$. The unitary stereographic projection operator between functions G in $L^2(S^2, d\Omega)$ and g in $L^2(\mathbb{R}^2, d^2\vec{x})$, and its inverse, respectively read

$$\begin{aligned}
[\Pi G](\vec{x}) &= \left(1 + \left(\frac{r}{2}\right)^2\right)^{-1} G\left(\pi^{-1}\vec{x}\right) \\
\left[\Pi^{-1} g\right](\omega) &= \left(1 + \tan^2 \frac{\theta}{2}\right) g(\pi\omega) ,
\end{aligned} \tag{2.9}$$

in spherical coordinates on the sphere $\omega = (\theta, \varphi)$, and polar coordinates on the plane $\vec{x} = (r, \varphi)$. The azimuthal coordinates on the plane and on the sphere are identified to one

---

[2]The operator L_Ψ in our notations coincides with the inverse of the standard frame operator A_Ψ defined in [5].

another: φ. The radial conformal diffeomorphism between points is given as $\pi(\theta, \varphi) = (r(\theta), \varphi)$ for $r(\theta) = 2\tan(\theta/2)$, and its inverse reads $\pi^{-1}(r, \varphi) = (\theta(r), \varphi)$ for $\theta(r) = 2\arctan(r/2)$. The diffeomorphism $r(\theta)$ and its inverse $\theta(r)$ explicitly define the stereographic projection and its inverse. This stereographic projection maps the sphere, without its South pole, on the entire plane: $r(\theta) : \theta \in [0, \pi[\rightarrow [0, \infty[$. Geometrically, it projects a point $\omega = (\theta, \varphi)$ on the sphere onto a point $\vec{x} = (r, \varphi)$ on the tangent plane at the North pole, co-linear with ω and the South pole (see Figure 1). The pre-factors in (2.9) are required to ensure the unitarity of the projection operators Π and Π^{-1}.
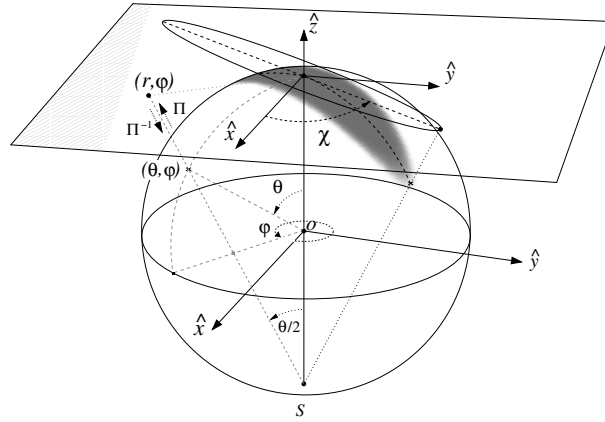

FIGURE 1   Stereographic projection π and its inverse π^{-1}, relating points (θ, φ) on the sphere and (r, φ) on its tangent plane at the North pole. The same relation holds through Π and Π^{-1} between functions living on each of the two manifolds, as illustrated by the shadow on the sphere and the localized region on the plane [29].

In this framework, the correspondence principle established states that, if the function $\psi(r, \varphi)$ in $L^2(\mathbb{R}^2, d^2\vec{x})$ satisfies the wavelet admissibility condition on the plane, i.e., essentially a zero-mean condition, then the function

$$\Psi(\theta, \varphi) = \left[\Pi^{-1}\psi\right](\theta, \varphi) \ , \tag{2.10}$$

in $L^2(S^2, d\Omega)$, satisfies the wavelet admissibility condition (2.8) on the sphere. This enables the construction of wavelets on the sphere by projection of wavelets on the plane. It also transfers wavelet properties from the plane onto the sphere, such as the steerability discussed in the next subsection.

2.3   Axisymmetric, Directional, and Steerable Wavelets

We present here axisymmetric, directional, and steerable wavelets on the sphere, built as inverse stereographic projections of wavelets on the plane.

An axisymmetric filter is by definition invariant under rotation around itself. That is, when located at the North pole, an axisymmetric filter is defined by a function $A(\theta)$ independent of the azimuthal angle φ. On the plane, the Mexican hat wavelet is defined as the normalized (negative) Laplacian of a Gaussian $e^{(x^2+y^2)/2}$. Its inverse stereographic projection defines the Mexican hat wavelet on the sphere (see Figure 2).
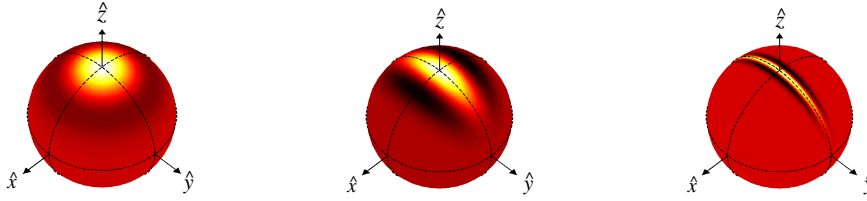
FIGURE 2 Mexican hat wavelet on the sphere for a dilation factor $a = 0.4$ and different eccentricities. On the left, the axisymmetric Mexican hat: $r = 1$ ($\epsilon = 0$) and $s = 2$ (left). At the center and on the right, respectively, the elliptical Mexican hat for $r = 0.5$ ($\epsilon \simeq 0.96825$) and $s = 2$, and $r = 0.1$ ($\epsilon = 0.99995$) and $s = 2$. Dark and light regions, respectively, identify negative and positive values.

Any non-axisymmetric filter is said to be directional, and is given as a general function $\Psi(\theta, \varphi)$ in $L^2(S^2, d\Omega)$. The elliptical Mexican hat wavelet is a directional modification of the axisymmetric Mexican hat, obtained by considering different widths σ_x and σ_y, respectively in the $\hat{x}$ and $\hat{y}$ directions on the plane for the original Gaussian: $e^{(x^2+y^2)/2} \rightarrow e^{(x^2/\sigma_x^2+y^2/\sigma_y^2)/2}$ [21]. The wavelet obtained as inverse stereographic projection of the normalized (negative) Laplacian of this Gaussian reads (see Figure 2) as:

$$\Psi^{(\text{mex})}(\omega) = \sqrt{\frac{2}{\pi}} N(\sigma_x, \sigma_y) \left(1 + \tan^2 \frac{\theta}{2}\right) \left[1 - \frac{4 \tan^2 \theta/2}{\sigma_x^2 + \sigma_y^2}\right.$$
$$\left.\left(\frac{\sigma_y^2}{\sigma_x^2} \cos^2 \varphi + \frac{\sigma_x^2}{\sigma_y^2} \sin^2 \varphi\right)\right] e^{-2 \tan^2 \frac{\theta}{2}\left(\cos^2 \varphi/\sigma_x^2 + \sin^2 \varphi/\sigma_y^2\right)}. \quad (2.11)$$

The constant $N(\sigma_x, \sigma_y) = (\sigma_x^2 + \sigma_y^2)[\sigma_x \sigma_y (3\sigma_x^4 + 3\sigma_y^4 + 2\sigma_x^2 \sigma_y^2)/2]^{-1/2}$ stands for the normalization. One can identify the wavelet parameters through the eccentricity of the ellipse defined by the points where the wavelet has zero value (zero-crossing), $\epsilon = (1 - (\sigma_x/\sigma_y)^4)^{1/2}$ (for $\sigma_y \geq \sigma_x$), and the sum $s = \sigma_x^2 + \sigma_y^2$. It is alternatively described by the ratio of the semi-major and semi-minor axes of the Gaussian $r = \sigma_x/\sigma_y$, and the sum $s = \sigma_x^2 + \sigma_y^2$. The axisymmetric Mexican hat is recovered for $\sigma_x = \sigma_y = 1$, in which case $r = 1$ ($\epsilon = 0$), and $s = 2$, and the normalization constant is unity, $N(\sigma_x, \sigma_y) = 1$.

On the plane, the real Morlet wavelet is a typical example of a directional wavelet. Its inverse stereographic projection on the sphere (see Figure 3) reads as (see also [9, 21] for similar projections):

$$\Psi^{(\text{mor})}(\omega) = \sqrt{\frac{2}{\pi}} N(k) \left(1 + \tan^2 \frac{\theta}{2}\right) \left[\cos\left(\frac{\vec{k} \cdot (\pi^{-1}\vec{x})}{\sqrt{2}}\right) - e^{-\vec{k}^2/4}\right]$$
$$e^{-2 \tan^2(\theta/2)}, \quad (2.12)$$

with $\pi^{-1}\vec{x} = (2 \tan(\theta/2) \cos \varphi, 2 \tan(\theta/2) \sin \varphi)$ in Cartesian coordinates. The arbitrary wave-vector $\vec{k} = (k_x, k_y)$ controls the direction and the frequency of oscillation of the wavelet ($\vec{k}^2 = k_x^2 + k_y^2$). The constant $N(k) = (1 + 3e^{-\vec{k}^2/2} - 4e^{-3\vec{k}^2/8})^{-1/2}$ stands for the normalization. Notice that for $|\vec{k}| = 2$, the real Morlet wavelet closely approximates at large scales to the second Gaussian derivative described in the following.

The notion of filter steerability was first introduced on the plane [13, 26], and more recently defined on the sphere [29]. Just as on the plane, a directional filter Ψ in $L^2(S^2, d\Omega)$
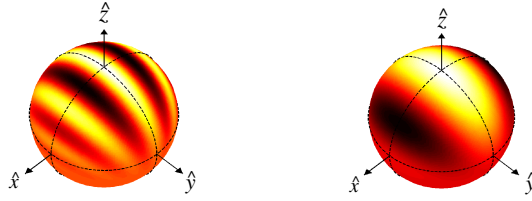
FIGURE 3   Real Morlet wavelet on the sphere for a dilation factor $a = 0.4$ and a wave-vector $\vec{k} = (6, 0)$ on the left, and for a dilation factor $a = 0.4$ and a wave-vector $\vec{k} = (2, 0)$ on the right. Dark and light regions, respectively, identify negative and positive values.

on the sphere is steerable if any rotation by $\chi \in [0, 2\pi[$ of the filter around itself $R^{\hat{z}}(\chi)\Psi$ may be expressed as a linear combination of a finite number of basis filters Ψ_m:

$$\left[R^{\hat{z}}(\chi)\,\Psi \right](\omega) = \sum_{m=1}^{M} k_m(\chi)\,\Psi_m(\omega) \ . \tag{2.13}$$

The weights $k_m(\chi)$, with $1 \leq m \leq M$, and $M \in \mathbb{N}$, are called interpolation functions. In particular cases, the basis filters may be specific rotations by angles χ_m of the original filter: $\Psi_m = R^{\hat{z}}(\chi_m)\Psi$. Steerable filters have a nonzero angular width in the azimuthal angle φ which makes them sensitive to a whole range of directions and enables them to satisfy the relation (2.13). In the spherical harmonics space, this nonzero angular width corresponds to an azimuthal angular band limit $N \in \mathbb{N}$ in the frequency index n associated with the azimuthal variable φ:

$$\widehat{\Psi}_{ln} = 0 \quad \text{for} \quad |n| \geq N \ . \tag{2.14}$$

Typically, the number M of interpolating functions is of the same order as the azimuthal band limit N.

    The derivatives of order N_d in direction $\hat{x}$ of radial functions on the plane are steerable wavelets. The transfer of the steerability property (2.13) from the plane to the sphere is obvious since the inverse stereographic projection is a radial operation, while the steerability only affects the azimuthal variable. The inverse stereographic projection of Gaussian derivatives therefore give steerable wavelets on the sphere. They may be rotated in terms of $M = N_d + 1$ basis filters, and are band-limited in φ at $N = N_d + 1$. We give the explicit examples of the normalized first and second Gaussian derivatives. A first derivative has a band limit $N = 2$, and only contains the frequencies $n = \{\pm 1\}$. It may be rotated in terms of two specific rotations at $\chi = 0$ and $\chi = \pi/2$, corresponding to the inverse projection of the first derivatives in directions $\hat{x}$ and $\hat{y}$, $\Psi^{\partial_{\hat{x}}}$ and $\Psi^{\partial_{\hat{y}}}$, respectively:

$$\left[R^{\hat{z}}(\chi)\,\Psi^{\partial_{\hat{x}}} \right](\omega) = \Psi^{\partial_{\hat{x}}}(\omega)\cos\chi + \Psi^{\partial_{\hat{y}}}(\omega)\sin\chi \ . \tag{2.15}$$

    The normalized first derivatives of a Gaussian (see Figure 4) in directions $\hat{x}$ and $\hat{y}$ read:

$$\Psi^{\partial_{\hat{x}}(\text{gau})}(\theta, \varphi) = \sqrt{\frac{8}{\pi}} \left(1 + \tan^2\frac{\theta}{2} \right) \tan\frac{\theta}{2} \cos\varphi\, e^{-2\tan^2(\theta/2)}$$

$$\Psi^{\partial_{\hat{y}}(\text{gau})}(\theta, \varphi) = \sqrt{\frac{8}{\pi}} \left(1 + \tan^2\frac{\theta}{2} \right) \tan\frac{\theta}{2} \sin\varphi\, e^{-2\tan^2(\theta/2)} \ . \tag{2.16}$$
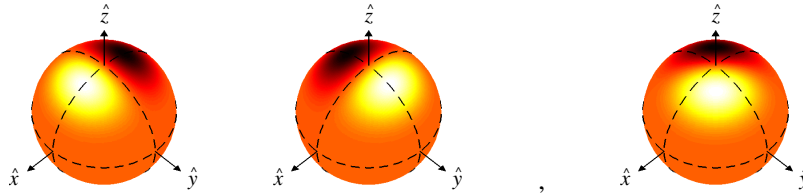
FIGURE 4 First Gaussian derivative wavelet on the sphere for a dilation factor $a = 0.4$: From left to right, $\Psi^{\partial_{\hat{x}}(\text{gau})}$, $\Psi^{\partial_{\hat{y}}(\text{gau})}$, and rotation by $\chi = \pi/4$ of $\Psi^{\partial_{\hat{x}}(\text{gau})}$. Dark and light regions, respectively, identify negative and positive values [29].

A second derivative has a band limit $N = 3$, and contains the frequencies $n = \{0, \pm 2\}$. It may be rotated in terms of three basis filters. It reads indeed in terms of the inverse projection of the second derivatives in directions $\hat{x}$ and $\hat{y}$, $\Psi^{\partial_{\hat{x}}^2}$ and $\Psi^{\partial_{\hat{y}}^2}$, respectively, and the cross derivative $\Psi^{\partial_{\hat{x}}\partial_{\hat{y}}}$ as:

$$\left[R^{\hat{z}}(\chi) \, \Psi^{\partial_{\hat{x}}^2} \right](\omega) = \Psi^{\partial_{\hat{x}}^2}(\omega) \cos^2 \chi + \Psi^{\partial_{\hat{y}}^2}(\omega) \sin^2 \chi + \Psi^{\partial_{\hat{x}}\partial_{\hat{y}}}(\omega) \sin 2\chi \, . \qquad (2.17)$$

The correctly normalized second derivatives of a Gaussian (see Figure 5) in directions $\hat{x}$ and $\hat{y}$ read:

$$\Psi^{\partial_{\hat{x}}^2(\text{gau})}(\theta, \varphi) = \sqrt{\frac{4}{3\pi}} \left(1 + \tan^2 \frac{\theta}{2} \right) \left(1 - 4 \tan^2 \frac{\theta}{2} \cos^2 \varphi \right) e^{-2 \tan^2(\theta/2)}$$

$$\Psi^{\partial_{\hat{y}}^2(\text{gau})}(\theta, \varphi) = \sqrt{\frac{4}{3\pi}} \left(1 + \tan^2 \frac{\theta}{2} \right) \left(1 - 4 \tan^2 \frac{\theta}{2} \sin^2 \varphi \right) e^{-2 \tan^2(\theta/2)}$$

$$\Psi^{\partial_{\hat{x}}\partial_{\hat{y}}(\text{gau})}(\theta, \varphi) = -\frac{4}{\sqrt{3\pi}} \left(1 + \tan^2 \frac{\theta}{2} \right) \left(\tan^2 \frac{\theta}{2} \sin 2\varphi \right) e^{-2 \tan^2(\theta/2)} \, . \qquad (2.18)$$
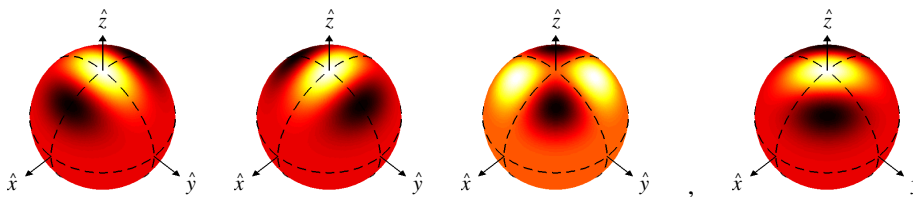

FIGURE 5 Second Gaussian derivative wavelet on the sphere for a dilation factor $a = 0.4$: From left to right, $\Psi^{\partial_{\hat{x}}^2(\text{gau})}$, $\Psi^{\partial_{\hat{y}}^2(\text{gau})}$, $\Psi^{\partial_{\hat{x}}\partial_{\hat{y}}(\text{gau})}$, and rotation by $\chi = \pi/4$ of $\Psi^{\partial_{\hat{x}}^2(\text{gau})}$. Dark and light regions, respectively, identify negative and positive values [29].

3. Directional Correlation

3.1 Directional and Standard Correlations

The directional correlation $\langle R\Psi | F \rangle$ of a function F with a filter Ψ is generically defined as the scalar product of the signal with all $SO(3)$ rotations of the filter [30]. It therefore lives

on $SO(3)$, and explicitly reads in $L^2(SO(3), d\rho)$ as:

$$\langle R(\rho)\Psi|F\rangle = \int_{S^2} d\Omega\, \Psi^*\left(R_\rho^{-1}\omega\right) F(\omega) \ . \tag{3.1}$$

As discussed in Section 2.1, if Ψ is the specific dilation of a wavelet on the sphere, the directional correlation coincides with the wavelet coefficients of the signal, at the corresponding scale [see relation (2.5)].

The standard correlation $\langle R_0\Psi|F\rangle$ of F with Ψ, is generically defined by the scalar product between the function F and the filter Ψ translated at any point $\omega_0 = (\theta_0, \varphi_0)$ on the sphere, but for a fixed direction, i.e., a fixed value $\chi = 0$. The result of the standard correlation explicitly gives a square-integrable function in $L^2(S^2, d\Omega)$ on the sphere:

$$\langle R(\omega_0)\Psi|F\rangle = \int_{S^2} d\Omega\, \Psi^*\left(R_{\omega_0}^{-1}\omega\right) F(\omega) \ . \tag{3.2}$$

The notation R_0 simply denotes a three-dimensional rotation with $\chi = 0$. It distinguishes the standard correlation $\langle R_0\Psi|F\rangle$ from the directional correlation $\langle R\Psi|F\rangle$ when the arguments are not specified.

Let us remark that, from relation (2.13), it explicitly appears that the directional correlation with a steerable filter Ψ reduces to a M-terms linear combination of standard correlations with the corresponding basis filters Ψ_m. In the particular case of an axisymmetric filter, there is no dependence at all of the correlation in the filter rotation χ. The directional correlation with an axisymmetric filter is therefore strictly equivalent to the standard correlation.

3.2 Pixelization and *a priori* Computation Cost

The directional and standard correlations are defined for square-integrable functions on a continuous variable $\omega = (\theta, \varphi)$ on the sphere. The translations and rotations of the filter also form a continuous variable $\rho = (\varphi_0, \theta_0, \chi) \in SO(3)$. Practical implementations are obviously based on a choice of discretization for each of these variables, i.e., a pixelization of S^2 and $SO(3)$. Let $N_p \simeq (2L)^2$ represent the number of sampling points ω in a given pixelization of S^2. The quantity $2L$ represents the mean number of sampling points in the position variables θ and φ, or θ_0 and φ_0. A simple extrapolation of the Nyquist-Shannon theorem on the line intuitively associates $L \in \mathbb{N}$ with the band limit, or maximum frequency, accessible on that pixelization in the "Fourier" indices conjugate to θ and φ for the signals and filters considered. For a sampling on $2L$ points in the direction χ the same band limit L is associated with the conjugate Fourier index. Notice that in the wavelet formalism, the dilation parameter $a \in \mathbb{R}_+^*$ must also be discretized for practical purposes.

Considering a simple quadrature, i.e., a discretization of the directional correlation integral, each scalar product on the sphere has an asymptotic complexity $\mathcal{O}(L^2)$. The overall asymptotic complexity for the directional correlation (3.1), taking into account all discrete $\rho = (\varphi_0, \theta_0, \chi)$ on $SO(3)$, is therefore of order $\mathcal{O}(L^5)$. We consider fine samplings of several megapixels on the sphere. To fix ideas, let us notice that the present NASA WMAP precision experiment on the CMB provides maps of the celestial sphere of around 3 megapixels. For a sampling associated with a band limit around $L \simeq 10^3$, the typical computation times for $(2L)^2$ multiplications and $(2L)^2$ additions are of order of 10^{-2} seconds on a standard processor. We take this value as a fair estimation of the computation time required for a scalar product. Consequently, a unique $\mathcal{O}(L^5)$ directional correlation would

take several years at that band limit on a single standard computer. Moreover, depending on the application, the directional correlation of multiple signals might be required. Typically, thousands of simulated signals are to be considered for a Monte Carlo statistical analysis. And for a wavelet analysis, multiple scales are to be considered for the filter. In conclusion, the directional correlation analysis of functions on the sphere is absolutely unaffordable for fine samplings with a band limit around $L \simeq 10^3$ in θ, φ, and χ. This conclusion remains when the use of multiple computers is envisaged. It is even strongly reinforced in the perspective of an analysis from finer pixelizations on the sphere. In particular, the forthcoming ESA Planck CMB experiment will provide 50 megapixels maps, i.e., $L \simeq 4 \times 10^3$.

The overall asymptotic complexity for the standard correlation, taking into account all discrete $\omega_0 = (\varphi_0, \theta_0)$ on S^2, is of order $\mathcal{O}(L^4)$. On a single standard computer, the corresponding computation time through simple quadrature, at a band limit $L \simeq 10^3$, would be of the order of days. Such a calculation still remains hardly affordable, particularly when multiple signals and multiple scales are considered.

3.3 Directional and Standard Correlations in Harmonic Space

The Wigner D-functions coefficients $\langle \widehat{R\Psi|F} \rangle^l_{mn}$ of the directional correlation $\langle R(\rho)\Psi|F \rangle$ living on $SO(3)$ are given as the pointwise product of the spherical harmonics coefficients $\widehat{F}_{lm}$ and $\widehat{\Psi}^*_{ln}$. The following correlation relation holds:

$$\langle R(\rho)\Psi|F \rangle = \sum_{l \in \mathbb{N}} \frac{2l+1}{8\pi^2} \sum_{|m|,|n| \leq l} \langle \widehat{R\Psi|F} \rangle^l_{mn} D^{l*}_{mn}(\rho) , \qquad (3.3)$$

with

$$\langle \widehat{R\Psi|F} \rangle^l_{mn} = \frac{8\pi^2}{2l+1} \widehat{\Psi}^*_{ln} \widehat{F}_{lm} . \qquad (3.4)$$

Indeed, the orthonormality of scalar spherical harmonics implies the Plancherel relation $\langle R\Psi|F \rangle = \sum_{l \in \mathbb{N}} \sum_{|m| \leq l} \widehat{R\Psi}^*_{lm} \widehat{F}_{lm}$. The action of the operator $R(\rho)$ on a function $G(\omega)$ in $L^2(S^2, d\Omega)$ on the sphere reads in terms of its spherical harmonics coefficients as: $[\widehat{R(\rho)G}]_{lm} = \sum_{|n| \leq l} D^l_{mn}(\rho)\widehat{G}_{ln}$. Inserting this last relation for Ψ in the former Plancherel relation finally gives the result.

The standard correlation $\langle R(\omega_0)\Psi|F \rangle$ lives on S^2 and could be decomposed in its spherical harmonics coefficients. However, for non-axisymmetric filters, these coefficients do not appear as a simple pointwise product similar to (3.4). The easiest way to express the standard correlation in harmonic space is therefore to simply consider the relations (3.3) and (3.4) with $\chi = 0$.

4. Fast Algorithms

4.1 Band-Limitation

The wavelet formalism defined in Section 2 holds for any signal and any wavelet satisfying the admissibility condition (2.8), irrespectively of any band-limitation consideration. However, the band-limitation represents a necessary condition for obtaining precise numerical implementations. We therefore consider band-limited functions G at some band limit $L \in \mathbb{N}$ on the sphere S^2, i.e., $\widehat{G}_{lm} = 0$ for $l \geq L$. From (3.4), the directional correlation of

a band-limited signal F by a band-limited filter Ψ, both with a band limit L on the sphere is thus also band-limited, with the same band limit: $\widehat{\langle R\Psi|F\rangle}^l_{mn} = 0$ for $l \geq L$.

In practice, the signals F may generally be very precisely approximated as band-limited, through considerations relative to the physical data acquisition process. For the typical wavelets described in Section 2, Ψ_a is also essentially band-limited, to very good approximation, provided that not too fine scales are considered ($a \nrightarrow 0$). Under these conditions, the wavelet coefficients of $W^F_\Psi (\rho, a)$ can therefore be calculated very precisely, or even exactly on equi-angular pixelizations, at suitable analysis scales. This is the scope of the fast directional correlational algorithms discussed in the next two subsections.

We do not consider here the question of the signal reconstruction from its wavelet coefficients through formula (2.7). The corresponding numerical implementation would require an explicit discretization of both the scales a and the $SO(3)$ variable ρ. First steps in that direction have been undertaken in [7].

4.2 Separation of Variables

The algorithm presented here for the directional correlation is based on the technique of separation of variables.

The factorized form (2.1) of the spherical harmonics naturally enables one to compute a direct spherical harmonics transform by separation of the integrations on the variables θ and φ. Conversely, an inverse transform may be computed as successive summations on the indices l and m, up to the band-limit L. Correctly ordering the corresponding operations provides a calculation of direct and inverse spherical harmonics transforms in $\mathcal{O}(L^3)$ operations [10]. This separation of variables for the spherical harmonics transforms may be performed on iso-latitude pixelizations on the sphere, i.e., pixelizations for which the sampling in θ is independent of φ, but where the sampling in φ may conversely depend on θ. This is the case for equi-angular pixelizations on the sphere. At a resolution $L \in \mathbb{N}, 2L \times 2L$ equi-angular pixelizations are defined by a uniform discretization in $2L$ samples both for the angles θ and φ. Such a pixelization scheme defines pixels with areas varying drastically with the co-latitude [31]. In particular, on a $2L \times 2L$ equi-angular grid, a sampling result on the sphere states that the spherical harmonics coefficients of a band-limited function with band-limit L may be computed exactly as a finite weighted sum, i.e., a quadrature, of the sampled values of that function [10]. HEALPix pixelizations (Hierarchical Equal Area iso-Latitude Pixelization) are also iso-latitude pixelizations, but where the sampling in φ explicitly depends on θ. Such a pixelization scheme defines $12N^2_{\text{side}}$ pixels of exactly equal areas, for a resolution parameter $N_{\text{side}} = 2^k$ with $k \in \mathbb{N}$. The computation of the spherical harmonics coefficients of a band-limited function is not theoretically exact on HEALPix grids, but can be made extremely precise by an iteration process [14]. These grids are notably used for the NASA WMAP CMB experiment and the ESA Planck CMB experiment.

The very same reasoning based on the factorized form (2.6) of the Wigner D-functions enables the calculation the inverse Wigner D-functions transform on $SO(3)$ required by (3.3) in $\mathcal{O}(L^4)$ operations [19, 20]. Considering an iso-latitude pixelization for the angles θ and φ on the sphere, the separation of variables for the Wigner D-functions transforms may be performed for any structure of the sampling in the third Euler angle χ, potentially depending on θ and φ. In particular, at a resolution parameter $L \in \mathbb{N}$, one may consider a uniform discretization in $2L$ samples for χ. Combined, for example, with an equi-angular pixelization at the same resolution for the angles θ and φ on the sphere, this defines a $2L \times 2L \times 2L$ equi-angular sampling in $\rho = (\varphi, \theta, \chi)$ on $SO(3)$.

Consequently, the algorithmic structure based on the separation of variables on iso-latitude pixelizations on the sphere may be summarized as follows. [18, 30] (a) Direct spherical harmonics transforms, $\widehat{\Psi}_{ln}$ and $\widehat{F}_{lm}$: $\mathcal{O}(L^3)$. (b) Correlation $\langle \widehat{R\Psi|F} \rangle_{mn}^{l}$ in harmonic space through (3.4): $\mathcal{O}(L^3)$. (c) Inverse Wigner D-functions transform $\langle R(\rho)\Psi|F \rangle$ on $SO(3)$ through (3.3): $\mathcal{O}(L^4)$. The global asymptotic complexity associated with the directional correlation is thus reduced from $\mathcal{O}(L^5)$ to $\mathcal{O}(L^4)$ thanks to the separation of variables. For band-limited signals and filters, the numerical precision of the algorithm is simply driven by the precision of computation of the spherical harmonics coefficients. It is therefore very precise on HEALPix grids notably, and theoretically exact on equi-angular pixelizations.

4.3 Factorization of Rotations

The following algorithm for the directional correlation is based on the technique of factor-ization of the three-dimensional rotations.

The three-dimensional rotation operators $R(\rho)$ on functions in $L^2(S^2, d\Omega)$ on the sphere may be factorized as [25, 28, 22]

$$R(\varphi_0, \theta_0, \chi) = R\left(\varphi_0 - \frac{\pi}{2}, -\frac{\pi}{2}, \theta_0\right) R\left(0, \frac{\pi}{2}, \chi + \frac{\pi}{2}\right) . \tag{4.1}$$

The directional correlation relation (3.3) and the expression (2.6) of the Wigner D-functions, matrix elements of the operators $R(\rho)$, therefore give an alternative expression for the directional correlation of arbitrary signals F and filters Ψ on the sphere. We get indeed

$$\langle R(\rho)\Psi|F \rangle = \sum_{m,m',n\in\mathbb{Z}} \langle \widehat{R\Psi|F} \rangle_{mm'n} e^{i(m\varphi_0 + m'\theta_0 + n\chi)} , \tag{4.2}$$

with the Fourier coefficients given by

$$\langle \widehat{R\Psi|F} \rangle_{mm'n} = e^{i(n-m)\pi/2} \sum_{l \geq C} d_{m'm}^{l}\left(\frac{\pi}{2}\right) d_{m'n}^{l}\left(\frac{\pi}{2}\right) \widehat{\Psi}_{ln}^{*} \widehat{F}_{lm} , \tag{4.3}$$

where $C = \max(|m|, |m'|, |n|)$, and with the symmetry relation $d_{m'm}^{l}(\theta) = d_{mm'}^{l}(-\theta)$ [27].

For a band-limited signal F and a band-limited filter Ψ with band limit $L \in \mathbb{N}$ on the sphere one has $|m|, |m'|, |n| \leq l < L$. The factorized form of the imaginary exponentials enables the calculation of the inverse three-dimensional imaginary exponentials transform required by (4.2) in $\mathcal{O}(L^4)$ operations. Just as for the Wigner D-functions transforms, considering an iso-latitude pixelization for the angles θ and φ on the sphere, the separation of variables for the three-dimensional imaginary exponentials may be performed for any structure of the sampling in the third Euler angle χ. In these terms, the directional cor-relation algorithm implemented on iso-latitude pixelizations for the angles θ and φ on the sphere through the factorization of rotations is structured as follows. (a) Direct spherical harmonics transforms, $\widehat{\Psi}_{ln}$ and $\widehat{F}_{lm}$: $\mathcal{O}(L^3)$. (b) Correlation $\langle \widehat{R\Psi|F} \rangle_{mm'n}$ in harmonic space through (4.3): $\mathcal{O}(L^4)$. (c) Inverse transform $\langle R(\rho)\Psi|F \rangle$ through (4.2): $\mathcal{O}(L^4)$. The global asymptotic complexity associated with the directional correlation is thus also reduced from $\mathcal{O}(L^5)$ to $\mathcal{O}(L^4)$ thanks to the factorization of rotations. [3] Again, for band-limited signals and filters, the numerical precision of the algorithm is simply driven by the precision of computation of the spherical harmonics coefficients.

---

[3]Notice that, while the Euler angles φ_0 and χ are in the range $\varphi_0, \chi \in [0, 2\pi[$, the original range for θ_0

4.4   Optimization with Steerable and Axisymmetric Filters

In terms of our rough estimations of Section 3.2, the separation of variables reduces the computation times on a standard computer from years to days for the directional correlation of band-limited signals and filters with band-limit $L \simeq 10^3$, typically sampled on megapixels maps. However, as already discussed, if a large number of simulations have to be analyzed, and at various scales of the filter, $\mathcal{O}(L^4)$ calculations remain hardly affordable even through the use of multiple computers.

Steerable filters are typically considered with a small number of interpolating functions M [see relation (2.13)], that is also a small azimuthal band-limit N [see relation (2.14)] relative to L. The use of such steerable filters further reduces the asymptotic complexity for the directional correlation. On the one hand, the directional correlation with a steerable filter Ψ reduces to a M-terms linear combination of standard correlations with the corresponding basis filters Ψ_m. For $M \ll L$, the asymptotic complexity of a directional correlation reduces to that of a standard correlation, with an *a priori* $\mathcal{O}(L^4)$ complexity, to which is simply added the $\mathcal{O}(L^3)$ linear combination which arises from (2.13). On the other hand, on iso-latitude pixelizations on the sphere, either the technique of separation of variables, or the factorization of three-dimensional rotations can be applied to the standard correlation, by setting $\chi = 0$ in the relations (3.3) or (4.2), respectively. For a steerable filter with a small azimuthal band limit $N \ll L$, the Fourier index n, with $|n| < N$, can be excluded from asymptotic complexity counts. It readily appears that the corresponding asymptotic complexity for the two algorithms hence reduces to $\mathcal{O}(L^3)$, on iso-latitude pixelizations on the sphere.[4] At $L \simeq 10^3$, our rough estimation of computation times is reduced from years to tens of seconds. This renders the computation easily affordable, even when multiple signals and multiple scales are considered.

Details on the algorithmic structure, computation times, memory requirements, and numerical stability of the corresponding implementations on HEALPix and equi-angular grids on the sphere may be found in [22] for the factorization of rotations, and in [30] for the technique of separation of variables and the optimization with steerable filters. Notice in that regard that a further optimization of the algorithm based on the separation of variables and with steerable filters may be achieved on equi-angular pixelizations on the sphere. It relies on the fact that Wigner D-functions transforms may be decomposed into linear combinations of spherical harmonics transforms, which therefore drive the overall asymptotic complexity for the directional correlation. On $2L \times 2L$ equi-angular pixelizations, these spherical harmonics transforms may be computed in $\mathcal{O}(L^2 \log^2 L)$ operations through the Driscoll and Healy algorithm [10, 15, 16], if the associated Legendre polynomials are pre-calculated. As discussed above, the sampling theorem on equi-angular pixelizations on the sphere also renders the calculation exact.

The axisymmetry of a filter $A(\theta)$ on the sphere is an extreme case of the steerability, for an azimuthal band limit $N = 1$: $\widehat{A}_{ln} = 0$ for $|n| \geq 1$. In that case, we already

---

is $\theta_0 \in [0, \pi]$, in order to cover the parameter space of $SO(3)$. Considering also $\theta_0 \in [0, 2\pi[$ puts the result on the parameter space of the three-torus $\mathbb{T}^3$, which covers twice the parameter space of $SO(3)$. In that context, the relation (4.2) is understood as a three-dimensional inverse Fourier transform, which can be calculated in $\mathcal{O}(L^3 \log_2 L)$ operations on a $2L \times 2L \times 2L$ equi-angular grid on $SO(3)$ by the use of the standard Cooley-Tukey fast Fourier transform algorithm. This optimization however does not reduce the overall asymptotic complexity for the directional correlation, still driven by the computation of (4.3) in $\mathcal{O}(L^4)$ operations.

[4]Let us remark that the issue of the sampling in χ is not relevant for steerable filters. The proper rotations by $\chi \in [0, 2\pi[$ are indeed analytically driven, and thus with infinite precision, by the relation (2.13).

emphasized that the proper rotation by χ has no effect on the filter and the directional correlation reduces to a standard correlation. At each scale, the wavelet coefficients of a signal with an axisymmetric filter therefore live on the sphere S^2 rather than on $SO(3)$. The directional correlation relation (3.4) consequently reduces to the following standard form, giving the spherical harmonics coefficients $\langle \widehat{R_0 A | F} \rangle_{lm}$ of the correlation of a signal F with an axisymmetric filter A as the pointwise product between the filter's Legendre coefficients $\widehat{A}_l$, and the spherical harmonics coefficients of the signal $\widehat{F}_{lm}$:

$$\langle \widehat{R_0 A | F} \rangle_{lm} = 2\pi \, \widehat{A}_l^* \, \widehat{F}_{lm} \; . \tag{4.4}$$

The correlation of a band-limited signal with a band-limited axisymmetric filter ($\widehat{A}_l = 0$ for $l \geq L$) is therefore readily computed in the harmonic space of S^2. On iso-latitude pixelizations on the sphere, the direct spherical harmonics transform of the signal, and the inverse spherical harmonics transform of the correlation, can simply be computed by separation of variables in the spherical harmonics. This provides an algorithmic structure with $\mathcal{O}(L^3)$ asymptotic complexity, which again can be reduced to $\mathcal{O}(L^2 \log^2 L)$ on equi-angular pixelizations.

5.   Conclusion

A new field of complex data processing has emerged in many areas of science. Scalar and tensor data, often distributed on nontrivial manifolds, come up at continually increasing resolutions. Powerful signal analysis techniques need to be developed to process such datasets.

In this article, we first reviewed recent formal developments for the continuous wavelet decomposition of signals on the sphere. Second, we detailed advances in the definition of the corresponding fast directional correlation algorithms.

These generic developments can find many applications in various fields such as computer vision (omnidirectional cameras, . . .), biomedical imaging (functional magnetic resonance imaging, . . .), geophysics (signals on the Earth's surface, . . .), or astrophysics and cosmology (signals on the celestial sphere, . . .). In that regard, the important results already obtained in cosmology through the wavelet analysis of the cosmic microwave background strongly illustrate the fact that the formalism developed represents a powerful tool for complex data processing on the sphere [23].

References

[1]   Abramowitz, M. and Stegun, I. (1965). *Handbook of Mathematical Functions,* Dover Publications Inc., New York.

[2]   Antoine, J.-P. and Vandergheynst, P. (1999). Wavelets on the 2-sphere: A group-theoretical approach, *Appl. Comput. Harmon. Anal.* **7**, 262.

[3]   Antoine, J.-P. and Vandergheynst, P. (1998). Wavelets on the n-sphere and related manifolds, *J. Math. Phys.* **39**, 3987.

[4]   Antoine, J.-P., Demanet, L., Jacques, L., and Vandergheynst, P. (2002). Wavelets on the sphere: Implementation and approximations, *Appl. Comput. Harmon. Anal.* **13**, 177.

[5]   Antoine, J.-P. and Vandergheynst, P. (2007). Wavelets on the two-sphere and other conic sections, *J. Fourier Anal. Appl.* **13**(4), 369–386.

[6]	Bennet, C. L., et al. (2003). First year Wilkinson Microwave Anisotropy Probe (WMAP) observations: Preliminary maps and basic results, *Astrophys. J. Suppl.* **148**, 1.

[7]	Bogdanova, I., Vandergheynst, P., Antoine, J.-P., Jacques, L., and Morvidone, M. (2005). Stereographic wavelet frames on the sphere, *Appl. Comput. Harmon. Anal.* **19**, 223.

[8]	Brink, D. M. and Satchler, G. R. (1993). *Angular Momentum,* 3rd ed., Oxford Clarendon Press.

[9]	Demanet, L. and Vandergheynst, P. (2003). Gabor wavelets on the sphere in, *Proc. SPIE Conference on Wavelets (Applications) in, Signal and Image Processing 5207*, Unser, M. A., Aldroubi, A., and Laine, A. F., Eds., 208 Bellingham, SPIE.

[10]	Driscoll, J. R. and Healy, D. M., Jr. (1994). Computing Fourier transforms and convolutions on the 2-sphere, *Adv. in Appl. Math.* **15**, 202.

[11]	Freeden, W. and Windheuser, U. (1996). Spherical Wavelet Transform and its Discretization, *Adv. Comput. Math.* **5**, 51.

[12]	Freeden, W., Gervens, T., and Schreiner, M. (1998). *Constructive Approximation on the Sphere, with Applications to Geomathematics,* Oxford Clarendon Press.

[13]	Freeman, W. T. and Adelson, E. H. (1991). The design and use of steerable filters, *IEEE Trans. Pattern Anal. Machine Intell.* **13**, 891.

[14]	Górski, K. M., Hivon, E., Banday, A. J., Wandelt, B. D., Hansen, F. K., Reinecke, M., and Bartelman, M. (2005). HEALPix—a framework for high resolution discretization, and fast analysis of data distributed on the sphere, *Astrophys. J.* **622**, 759.

[15]	Healy, D. M., Jr., Rockmore, D. N., Kostelec, P. J., and Moore, S. (2003). FFTs for the 2-sphere—improvements and variations, *J. Fourier Anal. Appl.* **9**(4), 341.

[16]	Healy, D. M., Jr., Kostelec, P. J., and Rockmore, D. N. (2004). Towards safe and effective high-order Legendre transforms with applications to FFTs for the 2-sphere, *Adv. in Comput. Math.* **21**, 59.

[17]	Holschneider, M. (1996). Continuous wavelet transforms on the sphere, *J. Math. Phys.* **37**, 8.

[18]	Kostelec, P. J. and Rockmore, D. N. (2003). FFTs on the rotation group, technical report (SFI-03-11-060).

[19]	Maslen, D. K. and Rockmore, D. N. (1997). Separation of variables and the computation of Fourier transforms on finite groups, I, *J. Amer. Math. Soc.* **10**, 169.

[20]	Maslen, D. K. and Rockmore, D. N. (1997). Generalized FFTs—a survey of some recent results in, *Proc. DIMACS Workshop on Groups and Computation 28* Finkelstein, L. and Kantor, W., Eds., 183, American Math. Soc., Providence, RI.

[21]	McEwen, J. D., Hobson, M. P., Lasenby, A. N., and Mortlock, D. J. (2005). A high-significance detection of non-Gaussianity in the WMAP 1-year data using directional spherical wavelets, *Monthly Not. Roy. Astron. Soc.* **359**, 1583.

[22]	McEwen, J. D., Hobson, M. P., Mortlock, D. J., and Lasenby, A. N. (2007). Fast directional continuous spherical wavelet transform algorithm, *IEEE Trans. Sign. Proc.* **55**, 520.

[23]	McEwen, J. D., Vielva, P., Wiaux, Y., Barreiro, R. B, Cayùn, L., Hobson, M. P, Lasenby, A. N, and Martínez-González, E. (2006). Cosmological applications of a wavelet analysis on the sphere, *J. Fourier Anal. Appl.* **13**(4), 495–510

[24]	The Planck collaboration (2005). Planck scientific programme (ESA Planck Blue book), technical report, (ESA-SCI(2005)1, astro-ph/0604069).

[25]	Risbo, T. (1996). Fourier transform summation of Legendre series and D-functions, *J. Geodesy* **70**, 383.

[26]	Simoncelli, E. P., Freeman, W. T., Adelson, E. H., and Heeger, D. J. (1992). Shiftable multiscale transforms, *IEEE Trans. Information Theory* **38**, 587.

[27]	Varshalovich, D. A., Moskalev, A. N., and Khersonskii, V. K. (1989). *Quantum Theory of Angular Momentum,* 1st ed., reprint, World Scientific, Singapore.

[28]	Wandelt, B. D. and Górski, K. M. (2001). Fast convolution on the sphere, *Phys. Rev. D* **63**, 123002.

[29]	Wiaux, Y., Jacques, L., and Vandergheynst, P. (2005). Correspondence principle between spherical and Euclidean wavelets, *Astrophys. J.* **632**, 15.

[30]	Wiaux, Y., Jacques, L., Vielva, P., and Vandergheynst, P. (2005). Fast directional correlation on the sphere with steerable filters, *Astrophys. J.* **652**, 820.

[31]	Wiaux, Y., Jacques, L., and Vandergheynst, P. (2005). Fast spin ± 2 spherical harmonics transforms and application in cosmology, preprint (astro-ph/0508514).

Signal Processing Institute, Ecole Polytechnique Fédérale de Lausanne (EPFL)
CH-1015 Lausanne, Switzerland
e-mail: yves.wiaux@epfl.ch

Astrophysics Group, Cavendish Laboratory, University of Cambridge
CB3 0HE Cambridge, UK
e-mail: mcewen@mrao.cam.ac.uk

Instituto de Física de Cantabria (CSIC-UC), E-39005 Santander, Spain,
and
Astrophysics Group, Cavendish Laboratory, University of Cambridge, CB3 0HE Cambridge, UK
e-mail: vielva@ifca.unican.es